

# Automatic Generation of Geometrically Parameterized Reduced Order Models for Integrated Spiral RF-Inductors

L. Daniel and J. White  
Department of Electrical Engineering and Computer Science  
Research Lab in Electronics  
Massachusetts Institute of Technology  
Cambridge, Massachusetts

## ABSTRACT

In this paper we describe an approach to generating low-order models of spiral inductors that accurately capture the dependence on both frequency and geometry (width and spacing) parameters. The approach is based on adapting a multiparameter Krylov-subspace based moment matching method to reducing an integral equation for the three dimensional electromagnetic behavior of the spiral inductor. The approach is demonstrated on a typical on-chip rectangular inductor.

**Index terms:** RF-inductor synthesis, RF-inductor design, RF inductor optimization, parameterized model order reduction, parameterized reduced order modeling, modeling.

## 1. INTRODUCTION

In order to provide product designers with inexpensive wireless connectivity, designers of mixed-signal integrated circuits are often including radio-frequency (RF) subsystems. Almost all of these RF subsystems make use of inductors, and for on-chip applications, these inductors are fabricated using spirals of aluminum or copper. Therefore, in order to optimize RF designs, designers and computer-aided design tools need accurate, but easily evaluated, models of the electrical behavior for these spiral inductors.

Analytically determining general and easily evaluated models for spiral inductors is difficult because inductor current-voltage characteristics are nonlinearly dependent on both semiconductor process parameters, such as dielectric constants and metal thickness, and design parameters such as metal width and spacing. Instead, the most reliable approach to accurately determining spiral inductor characteristics is to solve numerically Maxwell's equations on the three-dimensional inductor geometry associated with the process and design parameters of interest. However, numerical simulation is too computationally expensive to allow for design exploration. If it were possible to extract geometrically parameterized, but inexpensive to evaluate, models for the spiral inductors, then such models could be used for detailed optimization and synthesis of RF subsystems.

The idea of generating parameterized reduced-order models is not new, recent approaches have been developed for interconnect that focus on statistical performance evaluation [1, 2] and clock skew minimization [3]. One recently developed technique for generating geometrically parameterized models of physical systems assumed a linear dependence on the parameter, and was applied to reducing a discretized linear partial differential equation using a projection approach [4]. Resistor-capacitor (RC) models of in-

terconnect are linearly dependent on width and spacing parameters, at least for simplified models, and are typically reduced with respect to the Laplace transform parameter using projection approaches [5, 6, 7, 8, 9, 10, 11, 12, 13]. This fortuitous combination of attributes made generating geometrically-parameterized reduced-order models of RC interconnect a natural candidate to drive the development of projection-based multiparameter model reduction techniques [14, 15].

In this paper we extend the parameterized model reduction approach presented in [15] to the case of spiral inductor modeling, a more challenging application because the inductor's electrical characteristics are nonlinearly dependent on geometry parameters. We start in the next section by describing the electromagnetic model for spiral inductors and the linear projection-based multiparameter model reduction technique. In Section 4, we describe a simple fitting approach combined with parameter extension to convert the nonlinear dependence on a few geometry parameters in the electromagnetic model of the spiral inductor to a linearly dependent model over a larger number of parameters. Specifics of the procedure are given in Section 5, results for a rectangular spiral inductor are given in Section 6. Finally, conclusions and acknowledgments are given in Section 7.

## 2. BACKGROUND: A VOLUME INTEGRAL FORMULATION

In order to characterize accurately the quality factor and resonant frequency of a integrated circuit spiral inductor, it is necessary to properly account for the impact of the distributed capacitance, skin depth, and proximity effects. In one commonly used formulation which captures these relevant effects, described in [16, 17], conductor volume currents and surface charges satisfy the following system of integral-differential equations:

$$\frac{\mathbf{J}(\mathbf{r})}{\sigma} + j\omega \frac{\mu}{4\pi} \int_V \frac{\mathbf{J}(\mathbf{r}')}{|\mathbf{r} - \mathbf{r}'|} d\mathbf{r}' = -\nabla\phi, \quad (1)$$

$$\frac{1}{4\pi\epsilon} \int_S \frac{\rho(\mathbf{r}')}{|\mathbf{r} - \mathbf{r}'|} d\mathbf{r}' = \phi(\mathbf{r}), \quad (2)$$

$$\nabla \cdot \mathbf{J}(\mathbf{r}) = 0, \quad (3)$$

$$\hat{\mathbf{n}} \cdot \mathbf{J}(\mathbf{r}) = j\omega\rho(\mathbf{r}), \quad (4)$$

where  $V$  and  $S$  are the union of the conductor volumes and surfaces,  $\mathbf{J}$  is the unknown volume current distribution and  $\rho$  is the unknown conductor surface charge (diagrammed for a single conductor in

the top of Fig. 1). The scalar potential, denoted above as  $\phi$ , is unknown on all but external contact surfaces. The constants  $\mu$ ,  $\epsilon$ , and  $\sigma$  are the free space permeability, the free space permittivity, and the conductor conductivity respectively. Finally,  $\omega$  is the angular frequency of the conductor excitation.

There are many approaches to discretizing the system represented by (1), (2), (3), and (4). Standard piecewise constant, higher order, or frequency-dependent basis functions have been used to represent  $J$  and  $\rho$  [18, 16, 19, 20, 21, 22], and the basis function coefficients have been determined using both collocation and Galerkin methods applied to (1) and (2). There are also several choices for imposing the current and charge conservation conditions in (3) and (4) [16, 23, 24]. In this effort, we have used piece-wise constant basis functions to approximate both volume currents and surface charges as shown in the bottom of Fig. 1. In addition, (1) and (2) were enforced using a Galerkin condition and collocation condition respectively. Finally, we have imposed current and charge conservation using a mesh formulation as in [17, 25], leading to a set of algebraic equations in the Laplace transform domain:

$$\begin{bmatrix} M_f & M_p \end{bmatrix} \begin{bmatrix} R_f + sL_f & 0 \\ 0 & \frac{P}{s} \end{bmatrix} \begin{bmatrix} M_f^T \\ M_p^T \end{bmatrix} I_m(s) = V_m(s) \quad (5)$$

where  $s$  is the Laplace transform variable,  $R_f$ ,  $L_f$  and  $P$  are the resistance, partial inductance and coefficient of potential matrices respectively.  $I_m(s)$  is the vector of unknown mesh currents, and  $V_m(s)$  is the mostly zero vector of known mesh voltages. The sparse matrices  $M_f$  and  $M_p$  represent KVL equations which involve current-carrying filaments or charged panels respectively. Defining a state  $x$  including  $I_m$  and  $\phi$ , (where  $\phi = PM_p^T I_m/s$ ), and using a manipulation shown in [25] one can write (5) as a dynamical state space linear system

$$\begin{aligned} s\mathcal{L}x &= -\mathcal{R}x + Bu \\ y &= B^T x \end{aligned} \quad (6)$$

where

$$x = \begin{bmatrix} I_m \\ \phi \end{bmatrix} \quad (7)$$

$$\mathcal{L} = \begin{bmatrix} M_f L_f M_f^T & 0 \\ 0 & P^{-1} \end{bmatrix} \quad (8)$$

$$\mathcal{R} = \begin{bmatrix} M_f R_f M_f^T & M_p \\ -M_p^T & 0 \end{bmatrix} \quad (9)$$

$$B = \begin{bmatrix} V_{m,s} \\ 0 \end{bmatrix}. \quad (10)$$

### 3. BACKGROUND: MODEL ORDER REDUCTION FOR LINEARLY PARAMETERIZED SYSTEMS

Consider a parameterized system of equations

$$\begin{aligned} (E_0 + s_1 E_1 + \dots + s_p E_p)x &= Bu \\ y &= Cx. \end{aligned} \quad (11)$$

where  $u$  is the input,  $y$  is the output,  $x$  is the vector of internal “states” related to the input and output through matrices  $B$  and  $C$  respectively,  $s_1, \dots, s_p$  are  $p$  scalar parameters, and  $E_0, \dots, E_p$  are  $n \times n$  matrices. If the parameterized system represents a “dynamical” system, a subset of the parameters will be dependent on a Laplace transform parameter.

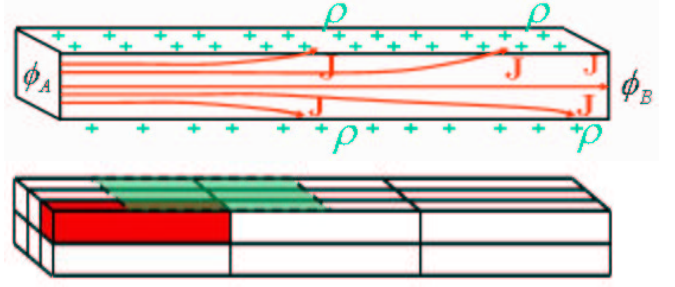


**Figure 1: Conductor volumes are discretized into current-carrying filaments to represent interior current distribution and conductors surfaces are discretized into charged panels to represent surface charge distribution.**

Following [15], one can produce a reduced order system using congruence transformations on the individual matrices  $E_0, \dots, E_p$

$$\begin{aligned} (V^T E_0 V + s_1 V^T E_1 V + \dots + s_p V^T E_p V) \hat{x} &= V^T B u \\ y &= C V \hat{x}, \end{aligned} \quad (12)$$

where  $\hat{x}$  is the reduced state vector of length  $q \ll n$ , and the projection matrix  $V$  has size  $n \times q$ . The columns of  $V$  can be chosen so that the transfer function of the reduced system (12) matches the first  $q$  terms of the multi-variable Taylor series expansion in  $s_1, \dots, s_p$  of the transfer function of the original system (11). Specifically, in [15] it is suggested that for a single-input multi-parameter system,  $V$  is constructed such that

$$\text{colspan}(V) = \text{span} \left\{ \bigcup_{m=0}^{m_q} \bigcup_{k_2=0}^{m-(k_p+\dots+k_3)} \dots \bigcup_{k_p=0}^m F_{k_2, \dots, k_p}^m(M_1, \dots, M_p) b \right\} \quad (13)$$

where vector  $b$  is given by

$$b = E_0^{-1} B,$$

and  $F_{k_2, \dots, k_p}^m(M_1, \dots, M_p)$  can be calculated recursively using (14), where matrices  $M_i$  are defined as

$$M_i = E_0^{-1} E_i \quad \text{for } i = 1, 2, \dots, p.$$

$$F_{k_2, \dots, k_p}^m(M_1, \dots, M_p) = \begin{cases} 0 & \text{if } k_i \notin \{0, 1, \dots, m\} \quad i = 2, \dots, p \\ 0 & \text{if } k_2 + \dots + k_p \notin \{0, 1, \dots, m\} \\ I & \text{if } m = 0 \\ M_1 F_{k_2, \dots, k_p}^{m-1}(M_1, \dots, M_p) + M_2 F_{k_2-1, \dots, k_p}^{m-1}(M_1, \dots, M_p) + \dots + M_p F_{k_2, \dots, k_{p-1}}^{m-1}(M_1, \dots, M_p) & \text{otherwise.} \end{cases} \quad (14)$$

#### 4. MODEL ORDER REDUCTION OF NON-LINEARLY PARAMETERIZED SYSTEMS

In this section we consider a non-linearly parameterized state space system model

$$\begin{aligned} \tilde{E}(s_1, \dots, s_\psi) x &= Bu \\ y &= Cx, \end{aligned} \quad (15)$$

where  $\tilde{E}(s_1, \dots, s_\psi)$  is a system descriptor matrix function of size  $n \times n$ , which in general may be non-linearly dependent on the  $\psi$  parameters  $s_1, \dots, s_\psi$ . These dependencies may be known analytically or a black box function evaluator, such as an electromagnetic field solver, may be used to compute  $\tilde{E}(s_1, \dots, s_\psi)$  for desired combinations of parameters  $s_1, \dots, s_\psi$ .

One way to reduce the order of such parameterized systems is to fit the nonlinear  $\tilde{E}$  with a linearly parameterized system as in (11), and then apply the moment-matching procedure described in Section 3. If  $\tilde{E}(s_1, \dots, s_\psi)$  is available in a simple analytical form, or if a field solver can be used to evaluate the function for many values of the parameters, then a least-squares polynomial interpolation scheme can be used to fit  $\tilde{E}$  to a truncated power series as in

$$\tilde{E}(s_1, \dots, s_\psi) = \tilde{E}_0 + \sum_r s_r \tilde{E}_r + \sum_{r,t} s_r s_t \tilde{E}_{r,t} + \sum_{r,t,l} s_r s_t s_l \tilde{E}_{r,t,l} + \dots \quad (16)$$

The nonlinearly dependent polynomial interpolant in (16) can then be cast in the form of (11) by extending the parameter set to  $p$  new parameters

$$s_i = \begin{cases} s_r & r = 1, \dots, \psi \\ s_r s_t & r = 1, \dots, \psi; t = 1, \dots, \psi \\ s_r s_t s_l & r = 1, \dots, \psi; t = 1, \dots, \psi; l = 1, \dots, \psi \\ \dots & \end{cases}$$

and consequently the  $p+1$  new matrices

$$E_i = \begin{cases} \tilde{E}_r & r = 0, \dots, \psi \\ \tilde{E}_{r,t} & r = 1, \dots, \psi; t = 1, \dots, \psi \\ \tilde{E}_{r,t,l} & r = 1, \dots, \psi; t = 1, \dots, \psi; l = 1, \dots, \psi \\ \dots & \end{cases}$$

The above simple scheme will only be effective for  $\tilde{E}$  matrix functions which are either only mildly nonlinear or functions of very few parameters. To see why, consider that following (16), the number of terms in a  $k^{th}$ -order power series approximation grows as  $O(\psi^k)$ , and therefore the approximating linearly parameterized system will have  $p = O(\psi^k)$  parameters. Matching moments for a large number of parameters is prohibitively expensive, though it is possible to improve complexity somewhat by exploiting the relationship between the power series approximation of  $\tilde{E}$  and moment-matching, along the lines of the single-parameter approach in [26].

#### 5. PARAMETERIZED MODEL REDUCTION OF AN SPIRAL RF-INDUCTOR

In this section we describe our procedure for generating parameterized low-order models of integrated spiral inductors. In this work, skin and proximity effects as well as resonances due to displacement currents (parasitic capacitors) are all accounted for using the method described in Section 2. A picture of the volume discretization is shown in Fig. 2

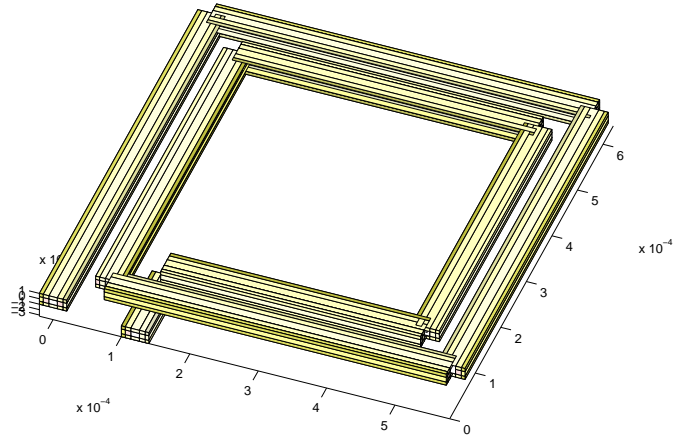


**Figure 2: Planar spiral two-turns RF-Inductor used for the analysis in this work. In this picture the volume discretization of the wires is made visible: the picture is not to scale. Different shades indicate different current densities in each filament.**

In order to keep the system sizes manageable for our prototype implementation, we did not include the effect of the substrate, although we recognize that it may play an important role in the behavior of many spiral inductors.

To construct a low-order parameterized dynamical linear system model for the two turn inductor as a function of wire width  $W$  and wire separation  $d$ , we followed a procedure based on the techniques presented above. In particular, we used the following steps:

1. We selected 9 evaluation points for wire width and wire separation

$$(W, d) \in \{(1\mu m, 1\mu m), (1\mu m, 3\mu m), (1\mu m, 5\mu m), (3\mu m, 1\mu m), (3\mu m, 3\mu m), (3\mu m, 5\mu m), (5\mu m, 1\mu m), (5\mu m, 3\mu m), (5\mu m, 5\mu m)\}$$

- Matrices  $R_f, L_f$ , and  $P$  in (5) depend on parameters  $W$  and  $d$ . For each pair  $(W_k, d_k)$  we used the solver in Section 2 to calculate the matrices  $R_f(W_k, d_k), L_f(W_k, d_k)$ , and  $P(W_k, d_k)$ . We then used (7) and (9) to calculate  $\mathcal{L}_k = \mathcal{L}(W_k, d_k)$  and  $\mathcal{R}_k = \mathcal{R}(W_k, d_k)$ . The discretization panels were adapted to represent charge crowding near edges and corners, and the filaments were adapted to accurately model current proximity and skin depth effects. For a two turn inductor, the number of filaments and panels required generated dense  $\mathcal{L}_k$  and  $\mathcal{R}_k$  matrices which were of size  $422 \times 442$ .
- We calculated a second order polynomial interpolation matching the 9 matrices data points  $\mathcal{L}_k$  and  $\mathcal{R}_k$  previously obtained for each pair of parameters  $(W_k, d_k)$  so that

$$\begin{aligned}\mathcal{L}(W, d) &\approx \mathcal{L}_{0,0} + W\mathcal{L}_{1,0} + d\mathcal{L}_{0,1} + W^2\mathcal{L}_{2,0} + Wd\mathcal{L}_{1,1} + d^2\mathcal{L}_{0,2} \\ \mathcal{R}(W, d) &\approx \mathcal{R}_{0,0} + W\mathcal{R}_{1,0} + d\mathcal{R}_{0,1} + W^2\mathcal{R}_{2,0} + Wd\mathcal{R}_{1,1} + d^2\mathcal{R}_{0,2}\end{aligned}$$

Specifically,  $\mathcal{L}_{r,t}^{i,j}$ , the  $(i, j)$  components of interpolation matrices  $\mathcal{L}_{r,t}$  can be calculated from  $\mathcal{L}_k^{i,j}$ , the  $(i, j)$  components of data matrices  $\mathcal{L}_k$  solving the least square problems

$$\begin{bmatrix} 1 & W_1 & d_1 & W_1^2 & W_1 d_1 & d_1^2 \\ 1 & W_2 & d_2 & W_2^2 & W_2 d_2 & d_2^2 \\ 1 & W_3 & d_3 & W_3^2 & W_3 d_3 & d_3^2 \\ 1 & W_4 & d_4 & W_4^2 & W_4 d_4 & d_4^2 \\ 1 & W_5 & d_5 & W_5^2 & W_5 d_5 & d_5^2 \\ 1 & W_6 & d_6 & W_6^2 & W_6 d_6 & d_6^2 \\ 1 & W_7 & d_7 & W_7^2 & W_7 d_7 & d_7^2 \\ 1 & W_8 & d_8 & W_8^2 & W_8 d_8 & d_8^2 \\ 1 & W_9 & d_9 & W_9^2 & W_9 d_9 & d_9^2 \end{bmatrix} \begin{bmatrix} \mathcal{L}_{1,0}^{i,j} \\ \mathcal{L}_{2,0}^{i,j} \\ \mathcal{L}_{0,1}^{i,j} \\ \mathcal{L}_{1,1}^{i,j} \\ \mathcal{L}_{0,2}^{i,j} \end{bmatrix} = \begin{bmatrix} \mathcal{L}_1^{i,j} \\ \mathcal{L}_2^{i,j} \\ \mathcal{L}_3^{i,j} \\ \mathcal{L}_4^{i,j} \\ \mathcal{L}_5^{i,j} \\ \mathcal{L}_6^{i,j} \\ \mathcal{L}_7^{i,j} \\ \mathcal{L}_8^{i,j} \\ \mathcal{L}_9^{i,j} \end{bmatrix}.$$

$\mathcal{R}_{r,t}^{i,j}$  the  $(i, j)$  components of interpolation matrices  $\mathcal{R}_{r,t}$  can be calculated from  $\mathcal{R}_k^{i,j}$ , the  $(i, j)$  components of data matrices  $\mathcal{R}_k$  solving similar least square problems. Other basis functions could be used for this interpolation.

- Assuming a Taylor series expansion point  $s_0$  for the the frequency variable  $s$  in (6) we introduced  $p = 11$  new parameters and we calculated the 12 matrices for the linearly parameterized system in (11)

$$\begin{array}{ll} s_1 = W & E_0 = s_0 * \mathcal{L}_{0,0} + \mathcal{R}_{0,0} \\ s_2 = d & E_1 = s_0 * \mathcal{L}_{1,0} + \mathcal{R}_{1,0} \\ s_3 = W^2 & E_2 = s_0 * \mathcal{L}_{0,1} + \mathcal{R}_{0,1} \\ s_4 = Wd & E_3 = s_0 * \mathcal{L}_{2,0} + \mathcal{R}_{2,0} \\ s_5 = d^2 & E_4 = s_0 * \mathcal{L}_{1,1} + \mathcal{R}_{1,1} \\ s_6 = s & E_5 = s_0 * \mathcal{L}_{0,2} + \mathcal{R}_{0,2} \\ s_7 = sW & E_6 = s_0 * \mathcal{L}_{0,0} \\ s_8 = sd & E_7 = s_0 * \mathcal{L}_{1,0} \\ s_9 = sW^2 & E_8 = s_0 * \mathcal{L}_{0,1} \\ s_{10} = sWd & E_9 = s_0 * \mathcal{L}_{2,0} \\ s_{11} = sd^2 & E_{10} = s_0 * \mathcal{L}_{1,1} \\ & E_{11} = s_0 * \mathcal{L}_{0,2} \end{array}$$

- Finally we applied the procedure in Section 3 and obtained a parameterized small system. For this example we chose to match one single moment with respect to each of the 11 parameters  $s_i$ , resulting in a final system as in (12) of order  $q = 12$  where each reduced matrix  $V^T E_i V$  is size  $12 \times 12$ . Note that matching a single moment with respect to the parameters  $s_i$  implies matching two moments in the original

parameters  $W$  and  $d$ . Note also that one can choose to adjust the accuracy with respect of each parameter  $s_i$  independently by adding more vectors related to  $s_i$  in (13).

## 6. EXAMPLE RESULTS

We have used the procedure described in the previous section to construct a parameterized low order model for a two-turn inductor. Wire width and wire separation were varied between 1um and 5um. The overall dimensions of the inductor is maintained constant at 600um x 600um. The wire thickness is 1um. The effect of the substrate is neglected. In Fig. 3 and 4 we show inductance and the quality factor of the inductor

$$\begin{aligned}L_{ind} &= \frac{\text{Im}\{Z_{ind}\}}{\omega} \\ Q_{ind} &= \frac{\omega L_{ind}}{R_{ind}} = \frac{\text{Im}\{Z_{ind}\}}{\text{Re}\{Z_{ind}\}},\end{aligned}$$

where  $Z_{ind} = 1/Y_{ind}$ , and  $Y_{ind}$  is the admittance of the inductor, captured by the transfer function of the dynamical state space linear system model. The original model (continuous lines) has order 422 while the reduced model after interpolation and congruence transformation has order 12 (dash-dotted lines). It can be observed how changing wire width and wire separations from 1um to 5um can have significant effects both on the quality factor of the inductor and on the position of the first resonance. The parameterized reduced order model produced by the procedure in Section 5 can successfully capture such dependency. It can also be observed that the interpolation step of the algorithm seems to be the most critical, since the largest errors (4% in amplitude near the peak for the quality factor, and 3% in position of the resonance peak for the inductance) are observed at  $d=2\text{um}$  and  $d=4\text{um}$ , which are far from the three interpolation data points at  $d=1\text{um}$ ,  $3\text{um}$  and  $5\text{um}$ .

## 7. CONCLUSIONS

In this paper we described a computational approach to generating low-order models of spiral inductors that accurately captures the linear dependence on frequency and the nonlinear dependence on geometry (width and spacing) parameters. The method began with a discretized integral equation to represent the electromagnetic behavior of the spiral inductor, and combined polynomial fitting with a multiparameter moment-matching technique to generate the parameterized reduced-order model. The approach was tested on a spiral inductor and used to reduce the order of the original discretization representation by a factor of 35, while still retaining good accuracy (worst case 4% error). The method has many limitations, most of them stemming from use of simple moment-matching for reduction and polynomial interpolation to fit the geometry dependence of the discretized integral equation matrices.

## 8. ACKNOWLEDGMENTS

The authors would like to thank Prof. Charles Sullivan (Dartmouth College) for useful discussion and feedback on design microfabricated RF inductors. Furthermore, the authors would like to acknowledge support from the MIT-Singapore Alliance, the Semiconductor Research Corporation, and the DARPA NeoCAD program managed by the Sensors Directorate of the Air Force Laboratory, USAF, Wright-Patterson AFB.

We would like to dedicate this paper to the memory of our valued colleague Professor Lee Kwok Hong.

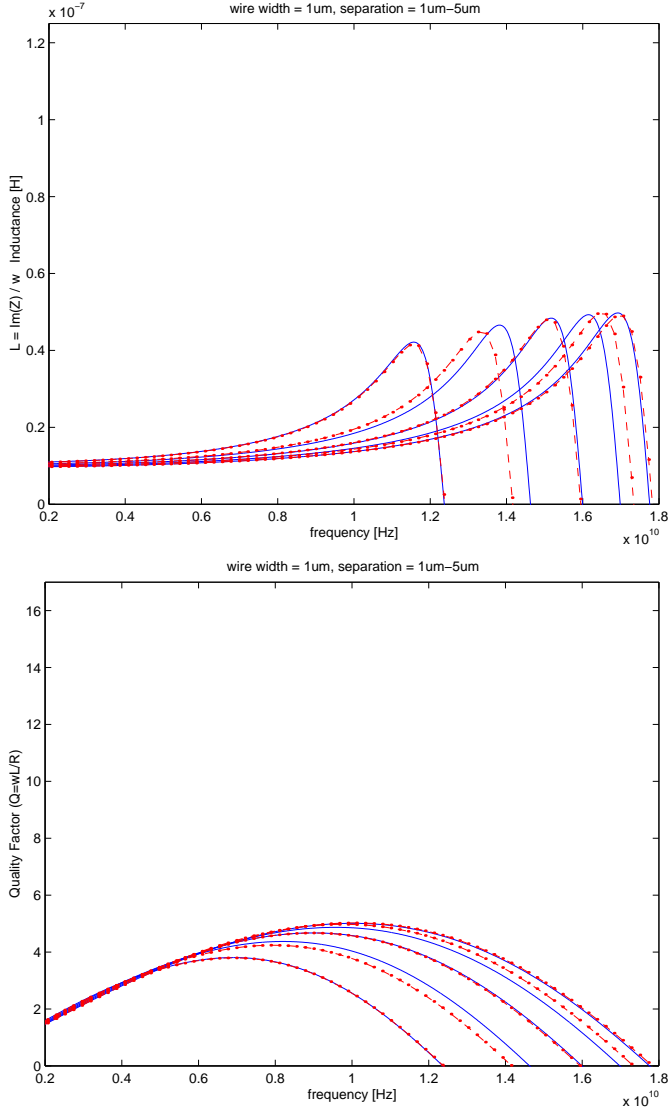


**Figure 3:** Above: inductance. Below: quality factor. The five continuous lines in each plot correspond to the response of the original model for the inductor in Fig. 2. The dash-dotted lines are the response of the parameterized reduced order model. The five pairs of curves correspond to wire width  $W=1\mu\text{m}$ , and wire separation  $d = 1\mu\text{m}, 2\mu\text{m}, 3\mu\text{m}, 4\mu\text{m}, 5\mu\text{m}$ .

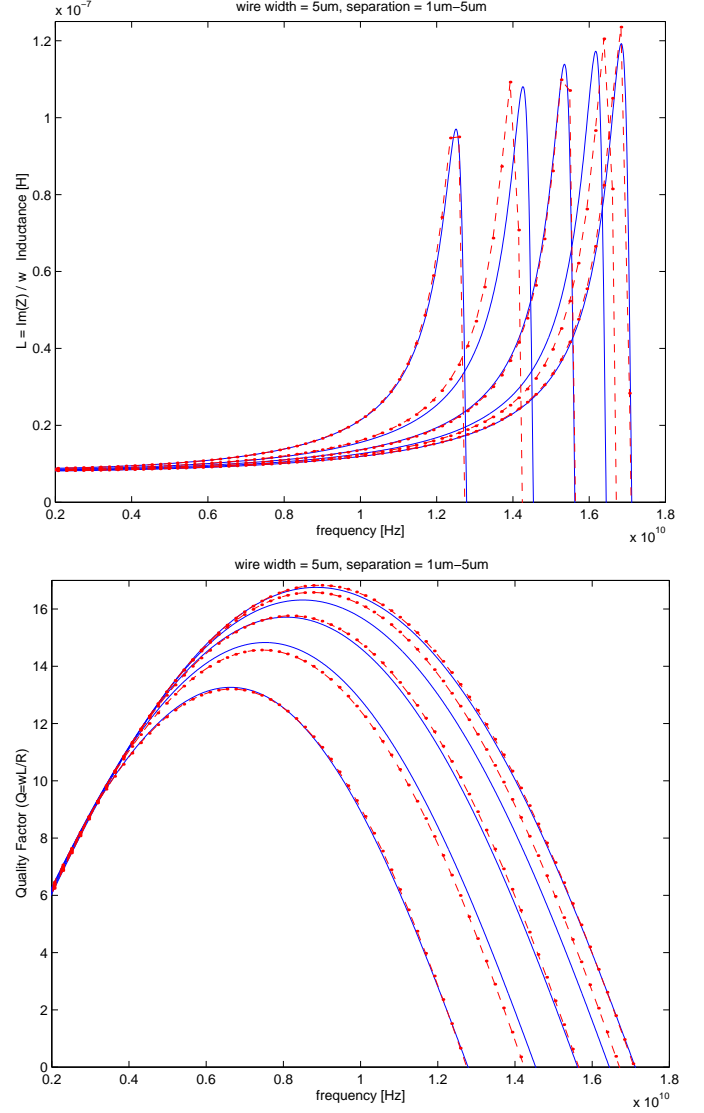


**Figure 4:** Same curves as in Fig. 3, obtained here for a different wire width  $W = 5\mu\text{m}$ . The largest errors (4% in amplitude near the peak for the quality factor, and 3% in position of the resonance peak for the inductance) are observed at  $d=2\mu\text{m}$  and  $d=4\mu\text{m}$ , which are farthest from the interpolation data points.

## 9. REFERENCES

- [1] Y Liu, Lawrence T. Pileggi, and Andrzej J. Strojwas. Model order-reduction of RCL interconnect including variational analysis. In *Proc. of the ACM/IEEE Design Automation Conference*, pages 201–206, New Orleans, Louisiana, June 1999.
- [2] P. Heydari and M. Pedram. Model reduction of variable-geometry interconnects using variational spectrally-weighted balanced truncation. In *Proc. of IEEE/ACM International Conference on Computer Aided-Design*, San Jose, CA, November 2001.
- [3] S. Pullela, N. Menezes, and L.T. Pileggi. Moment-sensitivity-based wire sizing for skew reduction in on-chip clock nets. *IEEE Trans. Computer-Aided Design*, 16(2):210–215, February 1997.
- [4] C. Prud'homme, D. Rovas, K. Veroy, Y. Maday, A.T. Patera, and G. Turinici. Reliable real-time solution of parametrized partial differential equations: Reduced-basis output bounds methods. *Journal of Fluids Engineering*, 2002.
- [5] K. Gallivan, E. Grimme, and P. Van Dooren. Asymptotic Waveform Evaluation via a Lanczos Method. *Applied Mathematics Letters*, 7(5):75–80, 1994.
- [6] Peter Feldmann and Roland W. Freund. Reduced-order modeling of large linear subcircuits via a block Lanczos algorithm. In *32<sup>nd</sup> ACM/IEEE Design Automation Conference*, pages 474–479, San Francisco, CA, June 1995.
- [7] K. J. Kerns, I. L. Wemple, and A. T. Yang. Stable and efficient reduction of substrate model networks using congruence transforms. In *Proc. of IEEE/ACM International Conference on Computer Aided-Design*, pages 207 – 214, San Jose, CA, November 1995.
- [8] Eric Grimme. *Krylov Projection Methods for Model Reduction*. PhD thesis, Coordinated-Science Laboratory, University of Illinois at Urbana-Champaign, Urbana-Champaign, IL, 1997.
- [9] I. M. Elfadel and David. L. Ling. A block rational arnoldi algorithm for multipoint passive model-order reduction of multiport RLC networks. In *Proc. of IEEE/ACM International Conference on Computer Aided-Design*, pages 66–71, San Jose, California, November 1997.
- [10] A. Odabasioglu, M. Celik, and L. T. Pileggi. PRIMA: passive reduced-order interconnect macromodeling algorithm. *IEEE Trans. Computer-Aided Design*, 17(8):645–654, August 1998.
- [11] L. M. Silveira, M. Kamon, I. Elfadel, and J. K. White. Coordinate-transformed arnoldi algorithm for generating guarantee stable reduced-order models of RLC. *Computer Methods in Applied Mechanics and Engineering*, 169(3-4):377–89, February 1999.
- [12] J. E. Bracken, D. K. Sun, and Z. Cendes. Characterization of electromagnetic devices via reduced-order models. *Computer Methods in Applied Mechanics and Engineering*, 169(3-4):311–330, February 1999.
- [13] A. C. Cangellaris and L. Zhao. Passive reduced-order modeling of electromagnetic systems. *Computer Methods in Applied Mechanics and Engineering*, 169(3-4):345–358, February 1999.
- [14] D. S. Weile, E. Michielssen, Eric Grimme, and K. Gallivan. A method for generating rational interpolant reduced order models of two-parameter linear systems. *Applied Mathematics Letters*, 12:93–102, 1999.
- [15] L. Daniel, C. S. Ong, S. C. Low, K. H. Lee, and J. K. White. Geometrically parameterized interconnect performance models for interconnect synthesis. In *International Symposium in Physical Design*, pages 202–207, San Diego, CA, USA, April 2002.
- [16] A. E. Ruehli. Equivalent circuit models for three dimensional multiconductor systems. *IEEE Trans. on Microwave Theory and Techniques*, 22:216–221, March 1974.
- [17] M. Kamon, N. Marques, and J. K. White. FastPep: a fast parasitic extraction program for complex three-dimensional geometries. In *Proc. of the IEEE/ACM International Conference on Computer-Aided Design*, pages 456–460, San Jose, CA, November 1997.
- [18] W. T. Weeks, L. L. Wu, M. F. McAllister, and A. Singh. Resistive and inductive skin effect in rectangular conductors. *IBM J. Res. Develop.*, 23(6):652–660, November 1979.
- [19] M. Kamon, M. J. Tsuk, and J. K. White. FASTHENRY: A multipole-accelerated 3-D inductance extraction program. *IEEE Trans. on Microwave Theory and Techniques*, 42(9):1750–8, September 1994.
- [20] K. Nabors and J. K. White. FastCap: a multipole accelerated 3-d capacitance extraction program. *IEEE Trans. on Computer-Aided Design of Integrated Circuits and Systems*, 10(11):1447–59, November 1991.
- [21] L. Daniel, A. Sangiovanni-Vincentelli, and J. K. White. Using conduction modes basis functions for efficient electromagnetic analysis of on-chip and off-chip interconnect. In *Proc. of the IEEE/ACM Design Automation Conference*, Las Vegas, June 2001.
- [22] L. Daniel, A. Sangiovanni-Vincentelli, and J. K. White. Techniques for including dielectrics when extracting passive low-order models of high speed interconnect. In *Proc. of the IEEE/ACM International Conference on Computer-Aided Design*, San Jose, CA, November 2001.
- [23] N. Marques, M. Kamon, J. K. White, and L. M. Silveira. A mixed nodal-mesh formulation for efficient extraction and passive reduced-order modeling of 3D interconnects. In *Proc. of the IEEE/ACM Design Automation Conference*, pages 297–302, San Francisco, CA, June 1998.
- [24] M. Kamon, N. Marques, L. M. Silveira, and J. K. White. Automatic generation of accurate circuit models. *IEEE Trans. on Components, Packaging, and Manufact. Tech.*, August 1998.
- [25] Mattan Kamon. *Fast Parasitic Extraction and Simulation of Three-dimensional Interconnect via Quasistatic Analysis*. PhD thesis, Massachusetts Institute of Technology, Cambridge, MA, January 1998.
- [26] J. R. Phillips, E. Chiprout, and D. D. Ling. Efficient full-wave electromagnetic analysis via model-order reduction of fast integral transforms. In *33<sup>rd</sup> ACM/IEEE Design Automation Conference*, pages 377–382, Las Vegas, Nevada, June 1996.